The wetting transition – *exploring liquids at an interface*

1 Introduction

The behaviour of liquids at interfaces and in confinement is a fascinating and important area of study. For example, the behaviour of a liquid under confinement between two surfaces determines how good a lubricant that liquid is. The nature of the interactions between the liquid and the surfaces is crucial. Consider, for example, the teflon coating on non-stick cooking pans, used because water does not adhere to (or **wet**) the surface. One can approach the problem from a mesoscopic fluid-mechanical point of view. However, if a microscopic approach is required, which relates the fluid properties at an interface to the nature of the molecular interactions, then one must start from statistical mechanics. There are a number of books such as Refs. [2, 3, 4, 5], which provide a good starting point. All of these include a discussion on a method called classical *density functional theory* (DFT), which is a theory for determining the density profile of a fluid in the presence of an external potential, such as that exerted by the walls of a container.

DFT is a statistical mechanical theory, where the aim is to calculate average properties of the system being studied. In statistical mechanics, the central quantity of interest is the partition function Z and once this is calculated, all thermodynamic quantities are given. However, Z a sum over all the possible configurations of the system, can rarely be evaluated exactly. Instead of focussing on Z, in DFT we seek to develop good approximations for the free energy. It can be shown that the free energy is a *functional* of the fluid density profile $\rho(\mathbf{r})$ and the equilibrium profile is that which minimises the free energy. Over the years, a great many different approximations for the free energy functionals have been developed, generally by making contact with results from other branches of liquid-state physics, as detailed in many lecture notes and review articles on the subject such as Refs. [6, 7, 8, 9, 10, 11, 12].

In this project we will start learning about the properties of inhomogeneous fluids by considering a simple lattice gas (Ising) model. This allows us to avoid much of the liquid-state physics and functional calculus that can be daunting for undergraduates when embarking on studying DFT and its applications. The advantage of starting from a lattice-gas model is that one can quickly develop a simple mean-field DFT (described below) and then proceed to calculate the bulk fluid phase diagram and study the interfacial properties of the model, determining the wetting behaviour, finding wetting transitions and all the other interesting phenomenology of liquids at interfaces. The computer algorithms required to solve these equations are fairly simple.

The aim of this Theory laboratory project is two-fold: (i) to derive the mean-field DFT

for an inhomogeneous lattice-gas fluid, whilst explaining the physics of the theory. The outline given here assumes the reader has had introductory statistical mechanics and thermodynamics courses, but little else beyond that. (ii) To illustrate the types of quantities that DFT can be used to calculate, such as the surface tension of the liquid-gas interface, to study wetting behaviour allowing us to answer the question "what is the shape of a drop of liquid on a surface?" These notes are accompanied by some *starter* computer code for numerical calculations written in both `Matlab` and `Python` to give you a guide, but you are free to write your code own in whatever language you prefer to solve the exercises.

2 Statistical mechanics of simple liquids

We consider a fluid composed of N atoms/molecules in a container. What follows is also relevant to colloidal suspensions and so we simply refer to the atoms, molecules, colloids, etc as 'particles'. The energy is a function of the set of position and momentum coordinates, $\mathbf{r}^N \equiv \{\mathbf{r}_1, \mathbf{r}_2, \ldots, \mathbf{r}_N\}$ and $\mathbf{p}^N \equiv \{\mathbf{p}_1, \mathbf{p}_2, \ldots, \mathbf{p}_N\}$ respectively, and is given by the Hamiltonian [5]

$$\mathcal{H}(\mathbf{r}^N, \mathbf{p}^N) = K(\mathbf{p}^N) + E(\mathbf{r}^N), \tag{1}$$

where K is the kinetic energy

$$K = \sum_{i=1}^{N} \frac{\mathbf{p}_i^2}{2m}, \tag{2}$$

and E is the potential energy due to the interactions between the particles and also to any external potentials such as those due to the container walls. When treating the system in the canonical ensemble, which has fixed volume V, particle number N and temperature T, the probability that the system is in a particular state is [5, 4, 13, 14]

$$f(\mathbf{r}^N, \mathbf{p}^N) = \frac{1}{h^{3N} N!} \frac{e^{-\beta \mathcal{H}}}{Z}, \tag{3}$$

where

$$Z = \frac{1}{h^{3N} N!} \int d\mathbf{r}^N \int d\mathbf{p}^N e^{-\beta \mathcal{H}}, \tag{4}$$

is the canonical partition function, h is Plank's constant and $\beta = (k_B T)^{-1}$ where k_B is Boltzmann's constant. The partition function allows macroscopic thermodynamic quantities to be related to the microscopic properties of the system which are defined in $\mathcal{H}$ (see below).

The kinetic energy contribution in Eq. (2), is solely a function of the momenta $\mathbf{p}^N$, and $E(\mathbf{r}^N)$, the precise form of which is yet to be defined, only depends on the positions of the particles $\mathbf{r}^N$. This allows the partition function in Eq. (4) to be simplified by performing the Gaussian integrals over the momenta to obtain

$$\begin{aligned} Z &= \frac{1}{h^{3N}} \int d\mathbf{p}^N e^{-\beta \sum_{i=1}^{N} \frac{\mathbf{p}_i^2}{2m}} Q = \frac{1}{h^{3N}} \int e^{-\beta \frac{\mathbf{p}_1^2}{2m}} d\mathbf{p}_1 \cdots \int e^{-\beta \frac{\mathbf{p}_N^2}{2m}} d\mathbf{p}_N Q, \\ &= \frac{1}{h^{3N}} \left(\sqrt{\frac{2m\pi}{\beta}} \right)^3 \cdots \left(\sqrt{\frac{2m\pi}{\beta}} \right)^3 Q = \left(\sqrt{\frac{2m\pi}{\beta h^2}} \right)^{3N} Q, \\ &= \Lambda^{-3N} Q, \end{aligned} \tag{5}$$

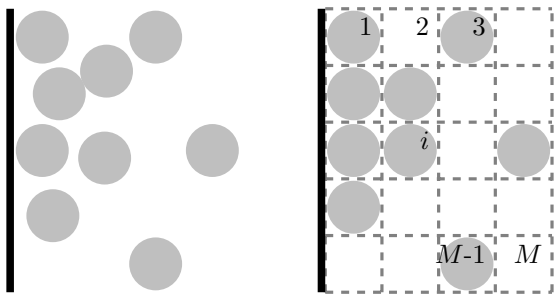

Figure 1: Illustration of how a free system, shown in (a), may be discretized in space by setting the particles on a lattice, shown in (b).

where $\Lambda = \sqrt{\beta h^2/2m\pi}$ is the thermal de Broglie wavelength and

$$Q = \frac{1}{N!}\int d\mathbf{r}^N e^{-\beta E}, \tag{6}$$

is the configuration integral [13]. Thus, the partition function is just the configuration integral multiplied by a factor Λ^{-3N} that depends on N, T and m, so the value of Λ is irrelevant for determining the state of the system. Changing Λ just adds a constant to the free energy per particle [see Eq. (10)] and so we safely assume $\Lambda = 1$.

Evaluating Q is the central problem here and, in general, this can not be done exactly and so approximations are required. In the following section we develop a simple lattice model approximation that allows progress. Note that the system described above has been analysed in the canonical ensemble. We discuss below how the system can instead be considered in the grand canonical ensemble.

3 Discrete model

3.1 Defining a lattice

We assume that the fluid is two dimensional (2D), to simplify the analysis. However, everything can easily be extended to a three dimensional (3D) system. We imagine a lattice discretises the space occupied by the fluid and so any configuration of particles may be described by a set of lattice occupation numbers $\{n_1, n_2, \ldots, n_N\} \equiv \{n_i\}$ which define if the lattice sites are filled ($n_i = 1$) or empty ($n_i = 0$) with n_i being the occupation number of site i. The width of each lattice site is set as σ, the diameter of a particle, and there are M sites. We set $\sigma = 1$ throughout and use this as our unit of length. The particles are assumed to be spherical, so that their orientation is not important. We now find that the configurational integral in Eq. (6) becomes a sum over the lattice sites. We will use the shorthand $i \equiv (k, l)$, where k and l are integer indices defining the x-y axis grid for our 2D lattice.

3.2 Energy of the system

To proceed, we must define the potential energy contribution to the Hamiltonian, E. We assume the following form

$$E = \sum_{i=1}^{M} n_i V_i - \frac{1}{2} \sum_{i,j} \epsilon_{ij} n_i n_j. \tag{7}$$

The first term is the contribution from the external potential V_i and the second term is the energy contribution from pair interactions between particles. We assume that there are no three-body or higher interactions. The interaction energy between particles at two lattice sites i and j is ϵ_{ij}. This value gets smaller as the distance between them increases and so ϵ_{ij} has the property that as $|i-j| \to \infty$, $\epsilon_{ij} \to 0$. The term $-\frac{1}{2}\sum_{i,j} \epsilon_{ij} n_i n_j$ denotes a sum over all pairs of lattice sites in the system, with the factor of $1/2$ correcting for double counting interactions. Allowing only pair interactions greatly simplifies the task of evaluating the partition function, but it can still be very arduous to evaluate this sum even for a moderately sized system. The probability of being in a particular configuration, $\{n_i\}$, for a fixed number of particles N, is now

$$P(\{n_i\}) = \frac{e^{-\beta E(\{n_i\})}}{Z}, \tag{8}$$

with the partition function defined as

$$Z = \sum_{\text{all states}} e^{-\beta E_{\text{state}}}, \tag{9}$$

where 'state' is a shorthand for a particular allowed set of occupation numbers $\{n_i\}$. Note the relation to the configuration integral in Eq. (6), since the sum over all states approximates the continuum integral $(N!)^{-1} \int d\mathbf{r}^N (\cdots)$.

3.3 Helmholtz free energy

The Helmholtz free energy is related to the partition function as follows [5, 13, 14]

$$F = -k_B T \ln Z. \tag{10}$$

All other thermodynamic quantities are obtained from derivatives of F. However, we are still unable to evaluate the sum in Eq. (9) and as a consequence can not calculate F. Under certain assumptions we can make some progress: consider the system where there is no external field, i.e. $V_i = 0$, and that $\epsilon_{ij} = 0$, so that the particles do not interact with each other. From Eq. (7), this gives $E = 0$ for all configurations and from Eq. (8) we observe that

$$P(\{n_i\}) = \frac{1}{Z}, \tag{11}$$

i.e. that all configurations are equally likely. From Eq. (9), we see that Z is just the number of possible states, which, for a system of M lattice sites containing N particles, is

$$Z = \frac{M!}{N!(M-N)!}. \tag{12}$$

For large systems, i.e. when both M and N are large, this can be simplified using Stirling's approximation, $\ln(N!) \approx N \ln N - N$, which, with Eq. (10), gives

$$F = -k_B T \left[M \ln M - N \ln N - (M - N) \ln(M - N) \right]. \tag{13}$$

The number density of particles in the system is $\rho = N/M$ (recall $\sigma = 1$) and so Eq. (13) gives

$$F = M k_B T \left[\rho \ln \rho + (1 - \rho) \ln(1 - \rho) \right]. \tag{14}$$

This homogeneous fluid has a uniform density ρ throughout. However, for an inhomogeneous fluid in the presence of a spatially varying external potential V_i we should expect the density to vary in space. The average density at lattice point i is defined as

$$\rho_i = \langle n_i \rangle, \tag{15}$$

i.e. it is the average value of the occupation number at site i, over all possible configurations: $\langle \cdots \rangle = \sum_{\text{all states}} (\cdots) P_{\text{state}}$. We now obtain an approximation for the free energy of the inhomogeneous fluid.

3.4 The grand canonical ensemble

We previously treated the system in the canonical ensemble with a fixed N, T and volume V (strictly, this is an area since the fluid is 2D but we refer to area as 'volume' throughout). Now we consider the system in the grand canonical ensemble with fixed V and T but allow N to vary by exchanging particles with a reservoir. The reservoir has a fixed chemical potential μ, and as the system is connected to this reservoir it has the same chemical potential (recall that the chemical potential is the energy required to insert a particle into the system). Physically, the easiest way to conceive the grand canonical ensemble is to imagine the system as being a subsystem of a much larger structure, with which it can exchange particles, and where the reservoir fixes T and μ in the subsystem.

The probability of a grand canonical system being in a particular state is [cf. Eq. (8)]

$$P(\{n_i\}) = \frac{e^{-\beta(E - \mu N)}}{\Xi}, \tag{16}$$

where the number of particles in the system is

$$N = \sum_{i=1}^{M} n_i.$$

The normalisation factor Ξ is the grand canonical partition function

$$\Xi = \operatorname{Tr} e^{-\beta(E - \mu N)}, \tag{17}$$

where the trace operator, Tr, is defined as

$$\operatorname{Tr} x = \sum_{\text{all states}} x = \sum_{n_1=0}^{1} \sum_{n_2=0}^{1} \cdots \sum_{n_M=0}^{1} x.$$

From the grand canonical partition function we can find the grand potential

$$\Omega = -k_B T \ln \Xi, \tag{18}$$

in an analogous manner to which the Helmholtz free energy is obtained in the canonical ensemble [cf. Eq. (10)]. The equilibrium state corresponds to the minimum of the grand potential.

3.5 Gibbs-Bogoliubov inequality

We now derive and then use the Gibbs-Bogoliubov inequality to show that there exists an upper bound on the free energy and finding the minimum of this bound gives an approximation to the true free energy.

Eq. (18) can be rearranged and equated to Eq. (17) to give

$$e^{-\beta\Omega} = \mathrm{Tr}\, e^{-\beta(E-\mu N)}. \tag{19}$$

The energy of a particular state E can be rewritten as

$$E = E_0 + E - E_0 = E_0 + \Delta E, \tag{20}$$

where E_0 is the energy of a reference system which we choose so as to be able to evaluate the partition function. We choose the system with $\epsilon_{ij} \equiv 0$ and $V_i \neq 0$. From Eqs. (19) and (20) we obtain

$$e^{-\beta\Omega} = \mathrm{Tr}\, e^{-\beta(E_0-\mu N)} e^{-\beta\Delta E}. \tag{21}$$

The statistical average value of any quantity x in the reference system is

$$\langle x \rangle_0 = \mathrm{Tr}\left(\frac{e^{-\beta(E_0-\mu N)}}{\Xi_0}\, x \right),$$

since $P_0 = e^{-\beta(E_0-\mu N)}/\Xi_0$ [see Eq. (16)]. So, from Eq. (21) we obtain

$$e^{-\beta\Omega} = e^{-\beta\Omega_0} \langle e^{-\beta\Delta E} \rangle_0, \tag{22}$$

with $\Xi_0 = e^{-\beta\Omega_0}$ given by Eqs. (17) and (18). Now, since e^{-x} is a convex function of x, then $\langle e^{-x} \rangle \geq e^{-\langle x \rangle}$ and from Eq. (22) we obtain the inequality

$$e^{-\beta\Omega} \geq e^{-\beta\Omega_0} e^{-\beta\langle \Delta E \rangle_0}. \tag{23}$$

Taking the logarithm of this gives the Gibbs-Bogoliubov inequality [5]

$$\Omega \leq \Omega_0 + \langle \Delta E \rangle_0. \tag{24}$$

This shows that there is an upper bound to the true grand potential Ω that depends solely on the properties of the reference system, and, more importantly, it allows us to find a 'best' approximation for Ω by minimising the right hand side of the inequality. We choose E_0 to depend upon parameters that may be varied and perform the minimisation with respect to variations in these parameters.

To proceed, we must define E_0. We choose

$$E_0 = \sum_{i=1}^{M} (V_i + \phi_i) n_i, \tag{25}$$

where V_i is the external potential, and ϕ_i are the parameters mentioned above, which are yet to be determined. Physically, they are the (mean field) additional effective potentials that attempt to capture (approximately) the average effect of the interactions between the particles.

The density at a particular lattice site is given by Eq. (15). Our (mean field) approximation for this quantity is

$$\rho_i = \langle n_i \rangle_0 = \mathrm{Tr}\left(\frac{e^{-\beta(E_0-\mu N)}}{\Sigma_0} n_i\right) = \frac{e^{-\beta(V_i+\phi_i-\mu)}}{1+e^{-\beta(V_i+\phi_i-\mu)}}. \tag{26}$$

Problem 1. *Work out the steps to arrive at Eq.* (26)*.*

Also, the reference system partition function is [cf. Eq. (17)]:

$$\Xi_0 = \mathrm{Tr}\, e^{-\beta(E_0-\mu N)} = \mathrm{Tr}\, e^{-\beta\sum_{i=1}^{M}(V_i+\phi_i-\mu)n_i} = \prod_{i=1}^{M}(1+e^{-\beta(V_i+\phi_i-\mu)}).$$

This may then be substituted into Eq. (18) to obtain the following expression for the grand potential

$$\Omega_0 = -k_B T \sum_{i=1}^{M} \ln(1+e^{-\beta(V_i+\phi_i-\mu)}). \tag{27}$$

Rearranging Eq. (26) to give $1-\rho_i = (1+e^{-\beta(V_i+\phi_i-\mu)})^{-1}$ and inserting it into Eq. (27) gives

$$\Omega_0 = k_B T \sum_{i=1}^{M} \ln(1-\rho_i). \tag{28}$$

By rewriting this as

$$\Omega_0 = k_B T \sum_{i=1}^{M} (\rho_i + 1 - \rho_i) \ln(1-\rho_i), \tag{29}$$

we can use Eq. (26) to express Ω_0 in the following form

$$\Omega_0 = k_B T \sum_{i=1}^{M} \left[\rho_i \ln \rho_i + (1-\rho_i)\ln(1-\rho_i)\right] + \sum_{i=1}^{M} (V_i + \phi_i - \mu)\,\rho_i. \tag{30}$$

Note that when $V_i = \phi_i = 0$, which corresponds to the case of a uniform fluid with $\epsilon_{ij} = 0$, this reduces to the result we saw earlier in Eq. (14), since $\Omega = F - \mu N$ [5, 18]. Returning to the general case $\epsilon_{ij} \neq 0$, from the definition of E_0 in Eq. (25), we find that $\Delta E = E - E_0$ is

$$\Delta E = -\frac{1}{2}\sum_{i,j} \epsilon_{ij} n_i n_j - \sum_{i=1}^{M} \phi_i n_i. \tag{31}$$

From Eq. (26), using $\rho_i = \langle n_i \rangle_0$ and Eq. (31), this then gives

$$\langle \Delta E \rangle_0 = -\frac{1}{2}\sum_{i,j} \epsilon_{ij} \rho_i \rho_j - \sum_{i=1}^{M} \phi_i \rho_i, \tag{32}$$

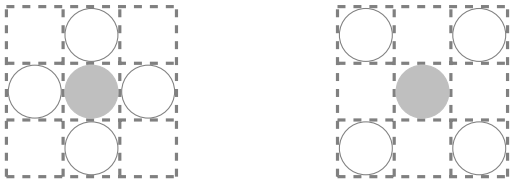

(a) (b)

Figure 2: The distinction between, (a), the nearest neighbors (open circles) to a particle (grey circle), and, (b), the next nearest neighbors.

where, because our reference system is non-interacting, we find that

$$\langle n_i n_j \rangle_0 = \langle n_i \rangle_0 \langle n_j \rangle_0 = \rho_i \rho_j.$$

Finally, Eqs. (30) and (32) can be used to obtain

$$\begin{aligned} \hat{\Omega} &= \Omega_0 + \langle \Delta E \rangle_0, \\ &= k_B T \sum_{i=1}^{M} [\rho_i \ln \rho_i + (1-\rho_i) \ln(1-\rho_i)] - \frac{1}{2} \sum_{i,j} \epsilon_{ij} \rho_i \rho_j + \sum_{i=1}^{M} (V_i - \mu) \rho_i. \end{aligned} \tag{33}$$

As discussed previously, this is an upper bound to the true grand potential Ω. One should choose the mean field $\{\phi_i\}$ so as to minimise $\hat{\Omega}$, in order to generate a best approximation for Ω. This is equivalent to choosing the set $\{\rho_i\}$ so as to minimise $\hat{\Omega}$, since the density ρ_i is defined by ϕ_i [cf. Eq. (26)]. What we have done here is to derive an approximate DFT for the lattice fluid. For DFT in general, one can prove that the equilibrium fluid density profile is that which minimises the grand potential functional [6].

4 Defining interactions and potentials

Up to this point, we have not specified the form of the potentials from the external field, or the particle interactions. We now define ϵ_{ij} and V_i.

4.1 Particle interactions

The term $-\sum_{i,j} \epsilon_{ij} \rho_i \rho_j$ in Eq. (33) represents the contribution to the free energy from the interactions between pairs of particles. A simple example of the continuum fluid we seek to model is made up of particles interacting via a Lennard-Jones pair potential [5] of the form

$$v(r) = \epsilon \left[\left(\frac{r_0}{r} \right)^{12} - 2 \left(\frac{r_0}{r} \right)^{6} \right], \tag{34}$$

where r is the distance between pairs of particles and r_0 is the distance at the minimum where $v(r_0) = -\epsilon$. Given that $v(2r_0) \approx -0.03\epsilon$, it is a good approximation to assume that each particle only interacts with the nearest and next nearest neighbouring particles, as illustrated in Fig. 2, and so we replace the particle interaction term in the free energy with

$$\sum_{i,j} \epsilon_{ij} \rho_i \rho_j \approx \epsilon_{nn} \sum_{i=1}^{M} \rho_i \sum_{j \,\mathrm{nn}\, i} \rho_j + \epsilon_{nnn} \sum_{i=1}^{M} \rho_i \sum_{j \,\mathrm{nnn}\, i} \rho_j, \tag{35}$$

where ϵ_{nn} and ϵ_{nnn} are the strengths of the interaction between nearest neighbour and next nearest neighbour particles, respectively. The term $\sum_{j\,\mathrm{nn}\,i}\rho_j$ denotes the sum of densities in lattice sites j which are the nearest neighbours to the site i. Similarly, $\sum_{j\,\mathrm{nnn}\,i}\rho_j$ denotes the sum over the next nearest neighbours. We now set $\epsilon_{nn}=\epsilon$ and $\epsilon_{nnn}=\epsilon/4$. This ratio $\epsilon_{nn}/\epsilon_{nnn}$ is not the value it would have if the Lennard-Jones potential were exactly applied but it is the optimum ratio to obtain circular drops when solved in two dimensions (see §9.2 below) [15, 16, 17]. Our definition captures the essence of the Lennard-Jones potential: the repulsive core is modelled by the onsite repulsion (one particle per lattice site) and the pair interaction terms crudely model the attractive forces. However, it is worth noting that even though the interaction energy between two well-separated ($r \gg r_0$) particles can be very small, the net contribution from all such long-range interactions may be significant and neglecting them may result in the theory failing to describe some interesting physics.

4.2 External potential

We assume that the interaction potential between a particle and the particles that form the wall of the container is of the Lennard-Jones form which decays for large r as $v(r)\sim -r^{-6}$. Summing the potential between a single fluid particle with all of the particles in the wall yields a net potential that decays as $V(y)\sim -y^{-3}$ for $y\to\infty$, where y is the perpendicular distance between the particle and the wall. We therefore assume that the wall exerts a potential of the form

$$V_i=\begin{cases}\infty & \text{if } k<1,\\ -\epsilon_w k^{-3} & \text{if } k\geq 1,\end{cases} \tag{36}$$

where ϵ_w is the parameter which defines the attractive strength of the confining wall. The integer index k is the distance, in the number of lattice sites, of the particle from the wall.

Problem 2. *Confirm the statement made above that assuming a Lennard-Jones potential for a wall in the x-z plane located at $y=0$ occupying all $y\leq 0$ gives a net potential $V(y)\sim -y^{-3}$ for $y\to\infty$ away from the wall.*

---

5 Research: the bulk fluid phase diagram

Before discussing the behaviour of the fluid at this wall, we first calculate the phase diagram of the bulk fluid using mean-field theory, away from the influence of any interfaces (this can be compared to the *Ising model* Theory laboratory project). When the temperature T is less than the critical temperature T_c, the fluid exhibits phase separation into a low density gas phase and a high density liquid phase. The *binodal* is the line in the phase diagram at which this transition occurs. Along the binodal, the liquid and the gas coexist in thermodynamic equilibrium, i.e. where the pressure, chemical potential and temperature of the liquid and gas phases are equal.

The lattice gas model has a particle-hole symmetry that is not present in a continuum description, but which is useful for calculating the binodal. This symmetry arises from the fact that if we replace $n_i=1-h_i$, where h_i is the hole occupation number, then the form of

Eq. (7) is unchanged. This symmetry leads to the density of the coexisting gas and liquid, ρ_g and ρ_l respectively, to be related as

$$\rho_l = 1 - \rho_g. \tag{37}$$

From Eq. (33) the Helmholtz free energy per lattice site, $f = F/M$, for a uniform fluid with density ρ, is

$$f = k_B T \left[\rho \ln \rho + (1-\rho)\ln(1-\rho)\right] - \frac{5\epsilon}{2}\rho^2. \tag{38}$$

Problem 3. *Show that the sum up to the next-nearest-neighbours interactions* $\sum_{i,j} \epsilon_{ij}\rho_i\rho_j = 5\epsilon\rho^2 M$ *and use this to confirm the result given in Eq. (38).*

The pressure in the system is [5, 19]

$$P(\rho) = -\left(\frac{\partial F}{\partial V}\right)_{T,N} = \rho\frac{\partial f}{\partial \rho} - f = -k_B T \ln(1-\rho) - \frac{5}{2}\epsilon\rho^2, \tag{39}$$

recalling that as we are working in 2D, the 'volume' is really an area, given by $V = M\sigma^2$. The binodal curve can be found by invoking Eq. (37) and solving $P(\rho) = P(1-\rho)$, giving

$$\frac{k_B T}{\epsilon} = \frac{5(2\rho - 1)}{2(\ln\rho - \ln(1-\rho))}, \tag{40}$$

which is displayed in Fig. 3a. The maximum on the binodal corresponds to the critical point, above which there is no gas-liquid phase separation. From the symmetry Eq. (37), the density at the critical point is $\rho = 1/2$ and the critical temperature is found to be $T_c = 5\epsilon/4k_B$.

The chemical potential can also be calculated from the Helmholtz free energy as [5, 19]

$$\mu(\rho) = \left(\frac{\partial F}{\partial N}\right)_{T,V} = \frac{\partial f}{\partial \rho} = k_B T \ln\left(\frac{\rho}{1-\rho}\right) - 5\epsilon\rho. \tag{41}$$

On substituting Eq. (40) into Eq. (41) we find that the chemical potential at coexistence is

$$\mu_{\text{coex}} = -\frac{5}{2}\epsilon, \tag{42}$$

which is displayed in Fig. 3b. The spinodal is also plotted in Fig. 3a. The *spinodal* denotes the locus in the phase diagram where the compressibility is zero, i.e. within this curve the fluid is unstable and spontaneous phase separation occurs. The spinodal is obtained from the following condition

$$\frac{\partial^2 f}{\partial \rho^2} = 0, \tag{43}$$

which, from Eq. (38), gives the following expression for the density dependence of the temperature along the spinodal,

$$\frac{k_B T}{\epsilon} = 5\rho(1-\rho), \tag{44}$$

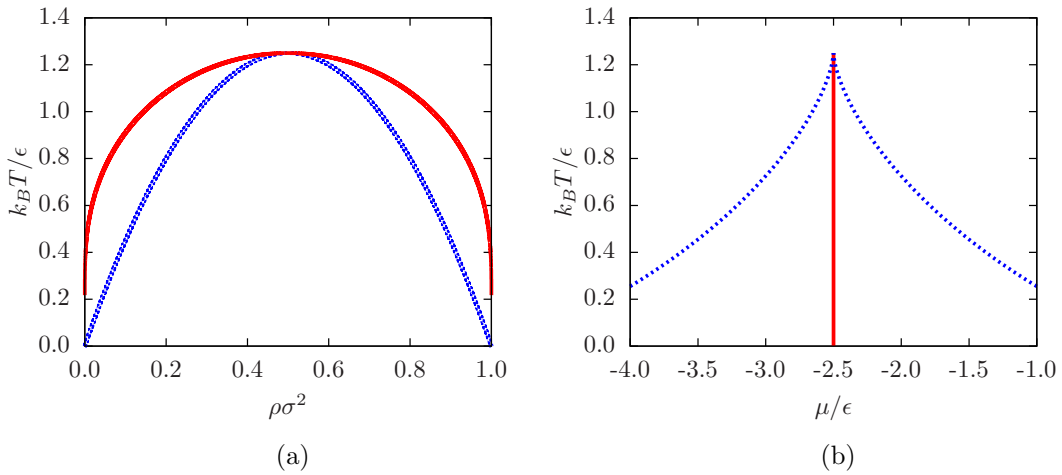

Figure 3: The bulk fluid phase diagram for the 2D lattice fluid. The solid red line is the binodal and the dashed blue line is the spinodal. In (a) we display the phase diagram in the dimensionless temperature k_BT/ϵ versus density plane and in (b) as a function of chemical potential.

also plotted in Fig. 3a. The spinodal can also be obtained as a function of μ from Eqs. (41) and (44). The result is displayed in Fig. 3b.

Problem 4. *How do the binodal, spinodal and critical temperature change for the case when there are only nearest neighbour interactions?*

---

6 Solving the bulk phase diagram numerically

Before moving on to an inhomogeneous fluid lets explore how to compute the phase diagram numerically. The equilibrium density profile is that which minimises $\hat{\Omega}$ in Eq. (33), under the assumption that $\rho_i = \rho$ and $V_i = 0$ for all sites i, so we need that

$$\frac{\partial \hat{\Omega}}{\partial \rho} = 0.$$

Performing this differentiation and rearranging gives the nonlinear equation for ρ,

$$\rho - (1-\rho)\exp\left[\beta\left(\mu + 5\epsilon\rho\right)\right] = 0. \tag{45}$$

We can find the phase diagram from this equation by solving for ρ as a function of the inverse temperature β and chemical potential μ. Depending on β, μ the solution will be $\rho \ll 1$, indicating a low density gas, or $\rho \approx 1$, indicating a high density liquid. For some regions there will be more than one solution, indicating instability.

Problem 5. *Fill in the gap to arrive at Eq. (45).*

Problem 6. *It is instructive to plot the lefthand side of Eq. (45) and observe how its roots vary with β and μ. Make a plot for $\beta\epsilon = 1$ with (i) $\mu/\epsilon = -3.0$, (ii) $\mu/\epsilon = -2.5$ and (iii) $\mu/\epsilon = -2.0$. Do the same for $\beta\epsilon = 2/3$. Comparing this to Fig. 3b comment on the plots.*

Beyond the graphical approach there several ways to solve Eq. (45) numerically allowing us to scan across the β-μ plane. One is to use a root finding algorithm, like Newton-Raphson, to locate the solutions, for example the `fzero` function in `Matlab` or `scipy.optimize.brentq` in the `Python` package `scipy`.

Problem 7. *Solve Eq. (45) numerically across the β-μ plane between $-5 \leq \mu/\epsilon \leq 0$ and $0 \leq 1/\beta\epsilon \leq 2$, making a plot like Fig. 3b, identifying the gaseous phase, liquid phase and unstable phase-separated region given by the spinodal.*

---

7 Liquids at an interface

We return now to the inhomogeneous fluid in the presence of an external potential. We will work with a 2D lattice of $L_x \times L_y$ sites and will consider how to solve for the density profile numerically.

7.1 An iterative method for calculating the density profile

As in the bulk case the equilibrium density profile is that which minimises $\hat{\Omega}$ in Eq. (33), i.e. it is the set $\{\rho_i\}$ that satisfies, for all i,

$$\frac{\partial \hat{\Omega}}{\partial \rho_i} = 0,$$

which in turn gives the set of coupled equations,

$$\rho_i = (1 - \rho_i) \exp\left[\beta\left(\mu + \epsilon \sum_{j \,\mathrm{nn}\, i} \rho_j + \frac{\epsilon}{4} \sum_{j \,\mathrm{nnn}\, i} \rho_j - V_i\right)\right]. \tag{46}$$

These equations can be solved iteratively for the profile $\{\rho_i\}$.

An initial approximation is required and the closer this is to the true solution, the better. We sometimes use $\rho_i = \exp(\beta(\mu - V_i))$, which is the exact result in the low density (ideal-gas) limit, or we may simply guess a likely profile. We can also use values from previous state points as an initial approximation when calculating at several state points successively, incrementing one parameter each time. With a suitable initial approximation for $\{\rho_i\}$, Eq. (46) can then be iterated until convergence is achieved.

It is often necessary during each iterative step to mix the result from evaluating the right hand side of Eq. (46), $\rho_i^{\rm rhs}$, in a linear combination with the result from the previous iteration $\rho_i^{\rm old}$, i.e.

$$\rho_i^{\rm new} = \alpha\rho_i^{\rm rhs} + (1-\alpha)\rho_i^{\rm old}, \tag{47}$$

where α may be small, typically in the range $0.01 < \alpha < 0.1$. This has the effect that only small steps are taken towards the minimum with each iteration. Omitting this mixing (i.e. $\alpha = 1$) can give a $\rho_i^{\rm new}$ that falls outside of the range (0,1) and once this happens the iterative routine breaks down.

Problem 8. *Implement an iterative solver of Eq.* (46) *and test that it works by applying it to a small 2D lattice, say size $L_x = 4$ and $L_y = 4$. Use periodic boundary conditions along the x and y axes, where the nearest neighbour of a lattice site on the boundary is taken to be the lattice site on the opposite boundary. Show that its recovers the bulk solutions obtained earlier for given β, μ from Problem 6.*

7.2 Boundary conditions for an interface

Let us now add a wall to our problem. At the wall, the boundary conditions (BC) for the density profile are straight forward: we simply set $\rho_i = 0$ for all lattice sites i 'inside' the wall – i.e. for $k < 1$ in Eq. (36). On the boundaries perpendicular to the wall, we normally use periodic BC. For the boundary opposite the wall, periodic BC in this situation would create an artificial substrate (i.e. so that the fluid is confined in a capillary, between two walls). This does not cause a problem in sufficiently large systems. However, a more efficient solution is to assume that the fluid is uniform with a fixed density beyond the boundary opposite the wall, with the specified density being that of the bulk gas solved earlier.

Problem 9. *Add to your 2D solver from Problem 8 an external potential V_i given by Eq.* (36) *modelling a wall at $y = 0$. Solve the density profile for $\beta\epsilon = 1.2$, $\beta\epsilon_w = 1.6$ with (i) $\mu/\epsilon = \mu_{\rm coex}/\epsilon - 1/6 \approx -2.67$ and (ii) $\mu/\epsilon = \mu_{\rm coex}/\epsilon - 1/30 \approx -2.53$. Use an $L_x = 4$ and $L_y = 20$ lattice, but with the density at the boundary away from the wall at $y = \sigma(L_y - 1)$ fixed at the gas bulk value ρ_g. Is L_y sufficiently large? Do we need to increase L_x?*

7.3 One dimensional model

So far, we have assumed for simplicity that the fluid is in 2D. However, since the density profile is defined as an average over all possible configurations [c.f. Eq. (15)], then if the external potential only varies in one direction [such as the potential in Eq. (36)], then so must the density profile. This is evident from the solutions to Problem 9, and is, of course, also the case for the 3D fluid. The equilibrium density profile must have the same symmetry as the external potential. For this reason we may reduce the DFT equations to be solved, Eq. (46), to a one-dimensional (1D) system, consisting of a line of lattice sites extending perpendicularly away from the wall. We do this by summing over the interactions in the

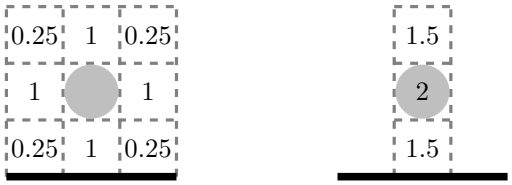

Figure 4: Illustration of the mapping of the full 2D particle pair interactions (a) onto an effective 1D system (b). The numbers represent the contribution towards the potential (in units of ϵ) from that particular lattice site with reference to the shaded particle in the centre. The 2D case on the left is that discussed above in §4.1 and on the right we display the resulting effective potential after mapping this system to 1D.

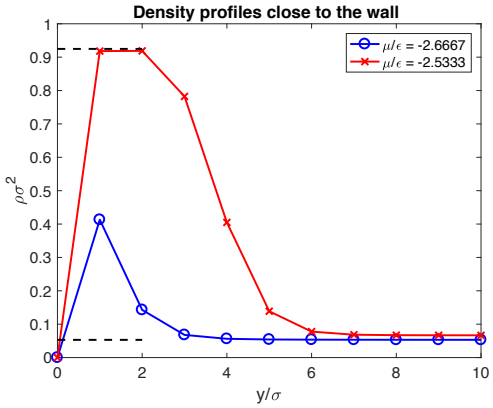

Figure 5: Density profiles along the y-axis away from the wall at $y = 0$ computed using the 1D effective model with $L_y = 20$ with the parameters given in Problem 9. The lower dashed line corresponds to the bulk densities ρ_g for (i) μ, while the upper one is ρ_l for (ii) μ from Problem 9.

(transverse) direction in which the density does not vary, as illustrated in Fig. 4. This maps the 2D system onto an effective 1D system with renormalised interactions between lattice sites and also introduces an effective on-site interaction[1]. A similar dimension reduction mapping can also be done for the 3D fluid.

Problem 10. *Implement the iterative solver for this effective 1D model and compare the results to the 2D solution from Problem 9. Make sure they agree and reproduce the density profiles shown in Fig. 5.*

---

8 Adsorption at the wall

Using the 1D effective model we will now produce lattice gas results which are typical of many full DFT calculations for a fluid exhibiting gas-liquid phase separation. Notice in

[1]Despite this, keep the 2D version for later when we will break the translational invariance along the x-axis.

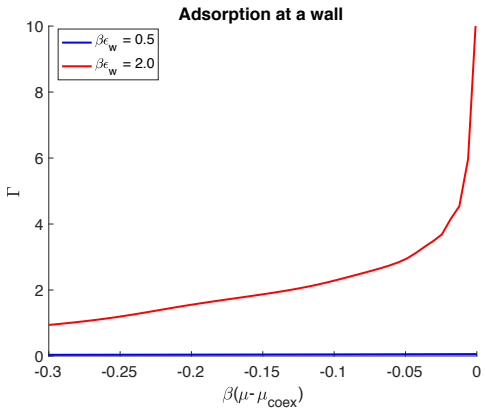

Figure 6: Adsorption Γ at a wall with μ approaching $\mu_{\rm coex}$ from below at a temperature $\beta\epsilon = 1.2$ for the interaction strength with the wall being $\beta\epsilon_w = 0.5$ and $\beta\epsilon_w = 2.0$.

Fig. 5 that as we approach $\mu_{\rm coex}$ the density around the wall climbs to a high density value expected of a liquid for a small region. This is a precursor to "wetting" the wall. To study this quantitively we shall look at the adsorption at the wall, which is defined as

$$\Gamma = \sum_{i \text{ along } y} (\rho_i - \rho_g), \tag{48}$$

where ρ_g is the bulk gas density for μ and β. From this we see that Γ measures the excess number of particles compared to the bulk (per unit length along the wall) in the direction perpendicular to the wall. By calculating results in the grand canonical ensemble, where particles are free to enter and leave the system, we can track how the adsorption changes with μ. A liquid is characterised as wetting a substrate when $\Gamma \to \infty$ as coexistence $\mu \to \mu^-_{\rm coex}$ is approached. Thus, at liquid-gas coexistence a macroscopically thick layer of the liquid forms between the gas and the substrate [20, 21, 22, 23, 24, 25, 26, 27]. Wetting only occurs when it is energetically beneficial, i.e. the liquid wetting the substrate is the state of least energy.

In Fig. 6 we illustrate how Γ, the adsorption at the wall, changes as the chemical potential is increased $\mu \to \mu^-_{\rm coex}$, to approach the coexistence value in Eq. (42), from below. When $\mu < \mu_{\rm coex}$ the bulk phase (away from the wall) is the gas phase, but for a wall to which the particles are attracted, the density at the substrate can be higher. As $\mu \to \mu^-_{\rm coex}$, the adsorption increases, either diverging[2] $\Gamma \to \infty$, when the liquid wets the wall, or remaining finite, when the liquid does not wet the wall. As T or ϵ_w are changed, there is often a phase transition from one regime to the other, termed the 'wetting transition'. The adsorption results in Fig. 6 are calculated for fixed $\beta\epsilon = 1.2$. When the strength of the attraction due to the wall is weak, $\beta\epsilon_w < 1$, the liquid does not wet the wall and the adsorption remains finite at coexistence, $\mu = \mu_{\rm coex}$. However, for stronger attraction, $\beta\epsilon_w > 1$, the wetting film thickness diverges as $\mu \to \mu^-_{coex}$.

[2]Numerically Γ won't diverge, but will instead increase to something of order 10, as shown in Fig. 6.

Problem 11. *Use your 1D solver to reproduce the adsorptions shown in Fig. 6 for weak attraction to the wall, $\beta\epsilon_w = 0.5$, and strong attraction to the wall, $\beta\epsilon_w = 2.0$.*

For large values of ϵ_w, like $\beta\epsilon_w = 2$ in Fig. 6, the adsorption diverges continuously. However, as we reduce $\beta\epsilon_w$ there can be a discontinuous jump in Γ as a result of crossing the so-called 'pre-wetting line' [20, 21, 22, 23, 24, 25, 26, 27]. These smaller jumps are 'layering transitions' and are due to an additional layer of particles being discontinuously added to the adsorbed liquid film. Such transitions are observed in more sophisticated DFT theories, however for the simplified lattice model used here leads unrealistic amplification of this effect due to the discretisation imposed.

Problem 12. *Plot the adsorption profiles, analogous to Fig. 6, but for $\beta\epsilon_w = 1.8$, $\beta\epsilon_w = 1.7$ and $\beta\epsilon_w = 1.6$. Do you see the emergence of a pre-wetting jump? Make a single plot of the density profiles for $\beta\epsilon_w = 1.6$ for an appropriate selection of μ's illustrating the discontinuous change due to pre-wetting.*

---

9 Wetting via droplet profiles and surface tensions

Tracking the adsorption is useful for understanding how the fluid behaves as coexistence is approached. However, it does not capture all facets of wetting behaviour. To do this we finish up this project by considering the formation of droplets of liquids on a surface. Specifically, we will treat the system canonically so that the total particle number $N = \sum_{i=1}^{M} \rho_i$ is fixed. We will also break translational symmetry along the x-axis by placing the centre of mass at the midpoint along the wall [28, 29].

9.1 Normalising the density profile

To describe an enclosed (canonical) system with fixed N, rather than being coupled to a particle reservoir which fixes μ, we can think of Eq. (33) as a constrained minimisation, i.e. as minimising the Helmholtz free energy

$$F = k_B T \sum_{i=1}^{M} \left[\rho_i \ln \rho_i + (1-\rho_i)\ln(1-\rho_i)\right] - \frac{1}{2}\sum_{i,j} \epsilon_{ij}\rho_i\rho_j + \sum_{i=1}^{M} V_i \rho_i, \tag{49}$$

subject to the constraint that

$$N = \sum_{i=1}^{M} \rho_i. \tag{50}$$

The chemical potential μ is then the Lagrange multiplier. To achieve this when iteratively calculating the density profile $\{\rho_i\}$, we modify the method described earlier in §7.1 so that

at each iteration following Eq. (47) the density profile is renormalised as $\rho_i^{\rm norm} = \mathcal{N}\rho_i^{\rm new}$, with

$$\mathcal{N} = N\left(\sum_{i=1}^{M}\rho_i^{\rm new}\right)^{-1},$$

so that the constraint in Eq. (50) is satisfied.

9.2 Droplet profiles

We now return to the full 2D model and aim to compute the density profiles corresponding to drops of liquid on a surface acting with the potential in Eq. (36). To do this we treat the system canonically, so Γ is fixed, and use an approximate initial profile for our iterative procedure consisting of setting the density to $\rho_i = \rho_g$ everywhere, apart from in a region in the middle of the system next to the wall, where we set $\rho_i = \rho_l$. The size of this region defines the size of the final liquid drop. A good choice is a fraction like 20% of the total system, and whatever the total particle number this corresponds to is then fixed by the normalisation described above. The boundary conditions are as described earlier in §7.2, with the wall at the bottom boundary, the left and right hand sides of the lattice having periodic boundary conditions and we fix $\rho_i = \rho_g$ along the top boundary.

In Fig. 7(a) we display an initial density profile used in the iterative solver, along with the final solution for $\beta\epsilon_w = 0.5$ in Fig. 7(b) and for $\beta\epsilon_w = 2.0$ in Fig. 7(c), both calculated on a 100×40 lattice for the fluid at an inverse temperature $\beta\epsilon = 1.2$. We can see that for the weak attraction $\beta\epsilon_w = 0.5$, where we found very little adsorption earlier, a droplet is formed on the surface, with a cross-sectional density profile shown in Fig. 7(d). In contrast for a strong attraction $\beta\epsilon_w = 2.0$ no drop is observed and instead a flat liquid film is formed. In fact the liquid drop spreads out more on the substrate as the value of ϵ_w increases. The contact angle θ that the drop makes with the substrate, as shown in Fig. 8, decreases as ϵ_w is increased, so that the drop becomes broader, until complete wetting occurs when $\beta\epsilon_w$ crosses the transition.

Problem 13. *Adapt your 2D code to work canonically as described in §9.1 and initialise it as specified in §9.2. Reproduce the plots shown for $\beta\epsilon_w = 0.5$ and $\beta\epsilon_w = 2$ in Fig. 7(b) and (c). Compute more plots showing how the droplet shape alters with $\beta\epsilon_w$, going from $\beta\epsilon_w = 0.1$ to $\beta\epsilon_w = 2$.*

9.3 Surface tension

The interfacial tension (or 'surface tension' in 3D) is the excess free energy due to the presence of an interface between two phase. In the present system there are three phases: the solid (wall), liquid and gas. Thus, there are three different interfacial tensions, for the wall-liquid, wall-gas and liquid-gas interfaces, γ_{wl}, γ_{wg} and γ_{lg}, respectively. For just the liquid and gas together, the interfacial tension γ_{lg} leads to a liquid drop surrounded by the gas to form a circle (in 2D, or a sphere in 3D), because this shape minimises the interfacial area and therefore its contribution to the free energy. When the wall is present, which can not change, the gas and liquid must arrange themselves so as to minimise the free energy. The resulting

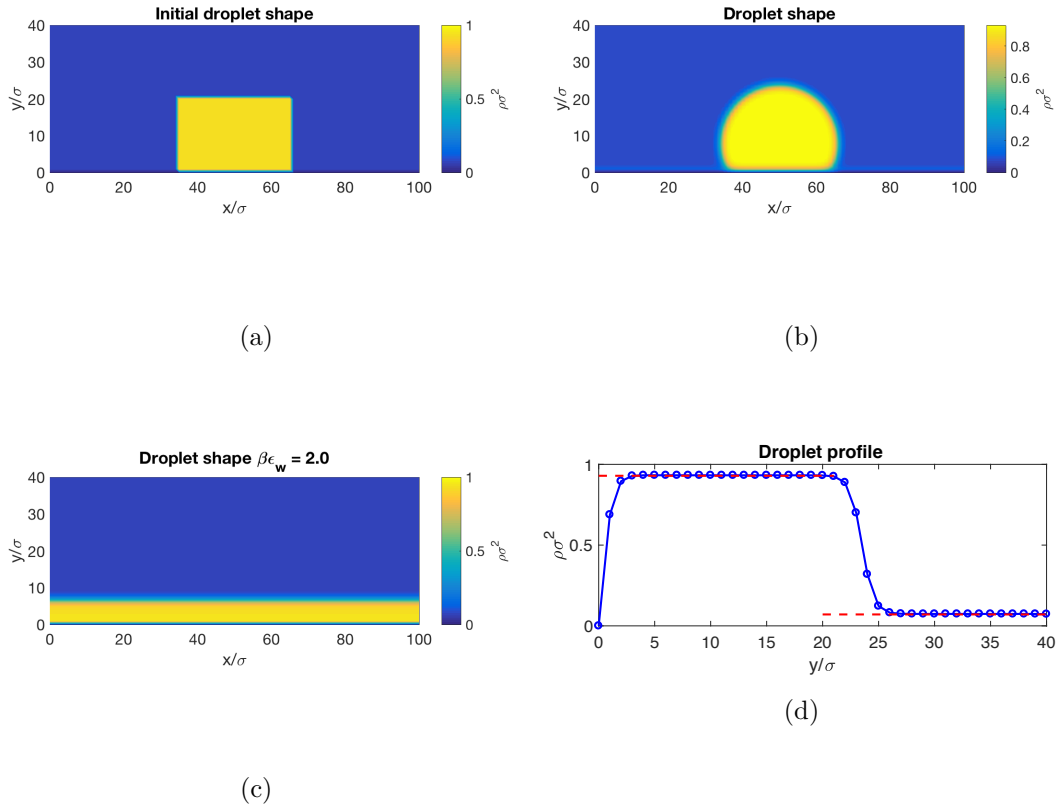

(a) (b) (c) (d)

Figure 7: The density profile of the initial state used in the iterative solver is shown in panel (a). The final solution for $\beta\epsilon = 1.2$ is shown for (b) $\beta\epsilon_w = 0.5$ and (c) $\beta\epsilon_w = 2.0$. A cut through the centre of the $\beta\epsilon_w = 0.5$ droplet displayed in panel (b) is shown in (d).

configuration depends on the values of the interfacial tensions. The equilibrium value of the contact angle is given by Young's Equation [20, 21, 22, 23, 24, 25]

$$\gamma_{lg} \cos\theta = \gamma_{wg} - \gamma_{wl}, \tag{51}$$

which can be understood by considering the balance of the forces due to the interfacial tensions, at the point where the three phases meet. Complete wetting only occurs when the sum $\gamma_{lg} + \gamma_{wl} \geq \gamma_{wg}$ so the real part of $\theta = 0$.

Problem 14. *For $\beta\epsilon = 1.2$ and an attraction to the wall $\beta\epsilon_w = 0.5$ is predicted to have a contact angle is $\theta = 115°$. Take the droplet density computed in Problem 13 for this ϵ_w, as shown in Fig. 7(b), and plot the density contour where $\rho = (\rho_l + \rho_g)/2$ along with the contact angle line as defined in Fig. 8. Is this prediction consistent?*

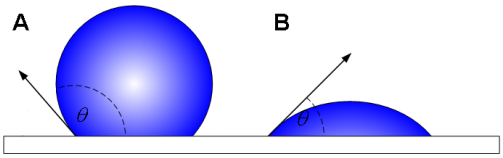

Figure 8: How the contact angle θ of a droplet on an interface is defined. For case A the angle is large, while for case B it is small.

10 Conclusions

We have presented a derivation of a simple lattice gas model DFT and discussed typical applications. Working with this model gives a reasonably hands-on introduction to many of the important ideas behind DFT and gives a platform to learn about different aspects of inhomogeneous fluids such as phase diagrams, adsorption and wetting. Studying this 'toy-model' gives a good insight into the physics of inhomogeneous liquids. Those of you who feel adventurous could go on to study the 'real thing' [2, 3, 4, 5, 6, 8, 9, 10, 11, 12] for final year or PhD projects.

Acknowledgements

This Theory laboratory project is based on the paper A. P. Hughes, U. Thiele and A. J. Archer "An introduction to inhomogeneous liquids, density functional theory, and the wetting transition", Am. J. Phys. **82** 1119 (2014). Consult this original paper and the references if you would like more details.

Appendix

Starter `Matlab` and `Python` code

For problems 6-8 some starter `Matlab` and `Python` code is provided in the **Blackboard** resources for this unit. This code demonstrates all of the basic features you need to solve all the problems in this project. You main task will be adapting it slightly, encapsulating bits of code into separate functions for easier re-use, and looping over them to generate plots over parameter spaces.

References

[1] P.-G. de Gennes, F. Brochard-Wyart and D. Queré, *Capillarity and Wetting Phenomena: Drops, Bubbles, Pearls, Waves* (Springer, 2004).

[2] D. Henderson (Ed.), *Fundamentals of Inhomogeneous Fluids* (CRC Press, 1992).

[3] J. S. Rowlinson, B. Widom, *Molecular Theory of Capillarity* (DOVER PUBN, 2002).

[4] H. Ted Davis, *Statistical Mechanics of Phases, Interfaces, and Thin Films* (Wiley-VCH, 1996).

[5] J.-P. Hansen and I. R. McDonald, *Theory of Simple Liquids*, Third Edition (Elsevier 2006).

[6] R. Evans, "The nature of the liquid-vapour interface and other topics in the statistical mechanics of non-uniform, classical fluids" Adv. Phys. **28** (2), 143–200 (1979).

[7] R. Evans, "Density Functionals in the Theory of Nonuniform Fluids" in *Fundamentals of Inhomogeneous Fluids*, 85–176, D. Henderson ed. (CRC Press, 1992).

[8] J. F. Lutsko, "Recent Developments in Classical Density Functional Theory", Adv. Chem. Phys. **144**, 1–92 (2010).

[9] J. Wu and Z. Li, "Density-Functional Theory for Complex Fluids", Annu. Rev.Phys. Chem. **58**, 85–112 (2007).

[10] J. Wu, "Density Functional Theory for Chemical Engineering: From Capillarity to Soft Materials", AIChE J. **52** (3) 1169–1193 (2006).

[11] P. Tarazona, J. A. Cuesta and Y. Martínez-Ratón "Density Functional Theories of Hard Particle Systems" , Lect. Notes Phys. **753** 247–341 (2008).

[12] H. Löwen, "Density Functional Theory for Inhomogeneous Fluids II (Freezing, Dynamics, Liquid Crystals)", Lecture Notes, 3rd Warsaw School of Statistical Physics, Warsaw University Press, 87–121 (2010).

[13] M. Plischke and B. Bergersen, *Equilibrium Statistical Mechanics*, Second Edition (World Scientific, 2006).

[14] L. E. Reichl, *A Modern Course in Statistical Physics*, Third Edition (Wiley, 2009).

[15] M. J. Robbins, "Describing colloidal soft matter systems with microscopic continuum models", PhD Thesis, Loughborough University, (2012).

[16] M. J. Robbins, A. J. Archer and U. Thiele, "Modelling the evaporation of thin films of colloidal suspensions using Dynamical Density Functional Theory", J. Phys.: Condens. Matter **23** 415102 (2011).

[17] S. Fomel and J. F. Claerbout, "Exploring three-dimensional implicit wavefield extrapolation with the helix transform", SEP report, **95** 43–60 (1997).

[18] D. Chandler, *Introduction to Modern Statistical Mechanics* (Oxford University Press, 1987).

[19] F. Mandl, *Statistical Physics* 2nd edition, (John Wiley & Sons, 1988).

[20] R. Evans, "Micoroscopic theories of simple fluids and their interfaces" in "Liquids at interfaces", Les Houches, Session XLVIII 1988, Ed. J. Charvolin, J.F. Joanney and J. Zinn-Justin (Elsevier 1989).

[21] M. Schick, "Introduction to Wetting Phenomena" in *Liquids at Interfaces, Proceedings of the Les Houches 1988 Session XLVIII*, 416–497, J. Charvolin, J.F Joanny and J. Zinn-Justin eds. (Elsevier 1990).

[22] S. Dietrich, "Wetting phenomena", in: Phase Transition and Critical Phenomena, vol.12, C. Domb and J.L. Lebowitz (Eds.), Academic Press, London (1988) pp. 2-218.

[23] D. Bonn and D. Ross, "Wetting transitions", Rep. Prog. Phys. **64**, 1085–1163 (2001).

[24] D. Bonn, J. Eggers, J. Indekeu, J. Meunier and E. Rolley, "Wetting and spreading", Rev. Mod. Phys. **81**, 739–805 (2009).

[25] V. M. Starov and M. G. Velarde, "Surface forces and wetting phenomena", J. Phys.: Condens. Matter **21**, 464121 (2009).

[26] A.O. Parry, "Three-dimensional wetting revisited", J. Phys.: Condens. Matter **8**, 10761–10778 (1996).

[27] E. Bruno, U.M.B. Marconi and R. Evans, "Phase transitions in a confined lattice gas: prewetting and capillary condensation", Physica **141A** 187–210 (1987).

[28] D. Reguera and H. Reiss, "The role of fluctuations in both density functional and field theory of nanosystems", J. Chem. Phys. **120**, 2558 (2004).

[29] A.J. Archer and A .Malijevsky, "On the interplay between sedimentation and phase separation phenomena in two-dimensional colloidal fluids", Mol. Phys. **109**, 1087 (2011).

[30] M. C. Stewart and R. Evans, "Wetting and Drying at a Curved Substrate: Long-Ranged Forces", Phys. Rev. E **71**, 011602–011615 (2005).